Briefings in Bioinformatics, 2025, **26(2)**, bbaf111
https://doi.org/10.1093/bib/bbaf111
Case Study

Disrupted microbial cross-feeding and altered L-phenylalanine consumption in people living with HIV

Hai Duc Nguyen [1] and Woong-Ki Kim[1,2,*]

[1]Division of Microbiology, Tulane National Primate Research Center, Tulane University, Covington, LA 70433, United States
[2]Department of Microbiology and Immunology, Tulane University School of Medicine, New Orleans, LA 70118, United States
*Corresponding author. Division of Microbiology, Tulane National Primate Research Center, Tulane University, Covington, LA 70433, United States.
E-mail: wkim6@tulane.edu

Abstract

This work aims to (1) identify microbial and metabolic alterations and (2) reveal a shift in phenylalanine production–consumption equilibrium in individuals with HIV. We conducted extensive searches in multiple databases [MEDLINE, Web of Science (including Cell Press, Oxford, HighWire, Science Direct, IOS Press, Springer Nature, PNAS, and Wiley), Google Scholar, and Embase] and selected two case–control 16S data sets (GenBank IDs: SRP039076 and EBI ID: ERP003611) for analysis. We assessed alpha and beta diversity, performed univariate tests on genus-level relative abundances, and identified significant microbiome features using random forest. We also utilized the MICOM model to simulate growth and metabolic exchanges within the microbiome, focusing on the Metabolite Exchange Score (MES) to determine key metabolic interactions. We found that L-phenylalanine had a higher MES in HIV-uninfected individuals compared with their infected counterparts. The flux of L-phenylalanine consumption was significantly lower in HIV-infected individuals compared with healthy controls, correlating with a decreased number of consuming species in the chronic HIV stage. *Prevotella*, *Roseburia*, and *Catenibacterium* were demonstrated as the most important microbial species involving an increase in L-phenylalanine production in HIV patients, whereas *Bacteroides*, *Faecalibacterium*, and *Blautia* contributed to a decrease in L-phenylalanine consumption. We also found significant alterations in both microbial diversity and metabolic exchanges in people living with HIV. Our findings shed light on why HIV-1 patients have elevated levels of phenylalanine. The impact on essential amino acids like L-phenylalanine underscores the effect of HIV on gut microbiome dynamics. Targeting the restoration of these interactions presents a potential therapeutic avenue for managing HIV-related dysbiosis.

Received: September 12, 2024. **Revised:** December 18, 2024. **Accepted:** February 25, 2025

Graphical Abstract

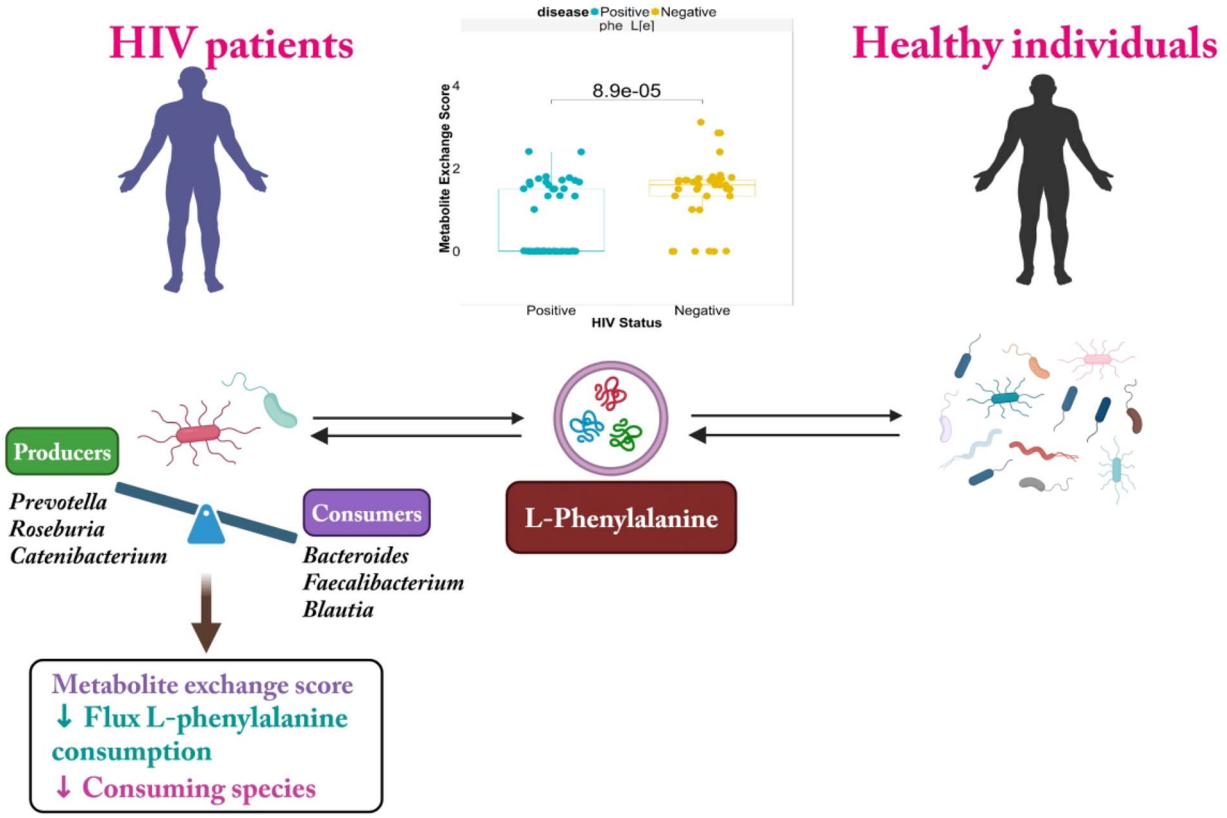

Keywords: HIV; microbiome; cross-feeding interactions; metabolic modeling; L-phenylalanine; metabolite exchange score

Introduction

The gut microbiome is essential for maintaining human health since it regulates a range of metabolic, immunological, and physiological functions [1, 2]. Microbial cross-feeding, where one microbial species generates metabolites that are subsequently utilized by other species, plays a crucial role in maintaining the stability of the gut microbiome [3]. These interactions are essential for nutrient cycling, immune regulation, and overall host health [3]. Disruptions in microbial interactions, such as the loss of microbial cross-feeding, can significantly impact the host's metabolism [4]. Disruptions in microbial cross-feeding can also lead to profound metabolic and immune system alterations, which are especially prominent in individuals living with HIV [5]. When these interactions are disrupted, particularly in HIV infection, microbial imbalances occur, leading to alterations in metabolic pathways. This imbalance can result in the loss of beneficial metabolites, like short-chain fatty acids, and the accumulation of harmful metabolites, such as pro-inflammatory molecules [6]. In HIV patients, these disruptions affect the metabolism of amino acids like phenylalanine, influencing immune function and metabolic health [7–9]. Understanding these disruptions helps to uncover the mechanisms behind disease progression and may guide therapeutic strategies to restore microbial balance and improve host metabolism.

HIV infection has been observed to induce substantial changes in the gut microbiota and alter its composition, which can subsequently impact the advancement of the disease and the general well-being of individuals infected with HIV [10]. These changes include an increase in harmful pathogenic bacteria and a decrease in beneficial butyrate-producing bacteria, which are crucial for preserving gut health and averting inflammation [11]. Furthermore, *Proteobacteria*, a phylum associated with inflammation, often exhibits an elevated presence in HIV-infected patients [12]. This heightened abundance of *Proteobacteria* contributes to both systemic inflammation and immunological activation. In HIV infection, there are also notable changes in microbial metabolites, which are the small molecules produced by the gut microbiota. These changes include a decrease in anti-inflammatory metabolites and phosphonoacetate, as well as an increase in pro-inflammatory molecules such as phenylethylamine and polyamines [5]. These metabolic alterations are crucial because they not only indicate the condition of the microbiome but also play a critical role in regulating immune responses and preserving the integrity of the intestinal barrier. Therefore, identifying the interactions between the microbiome and metabolites in HIV patients provides new insights toward better understanding the pathogenesis of HIV infection.

A growing body of research suggests that microbial cross-feeding, wherein gut microbes exchange metabolites, is disrupted in HIV infection, leading to altered metabolic profiles and immune activation [5]. This pioneering study explores the critical role of microbial cross-feeding interactions in gut health and their disruption in individuals living with HIV, contributing to our understanding of disease pathology and potential therapeutic avenues. We used the advanced MICOM model to simulate growth and metabolic exchanges within the microbiome, with

a particular focus on Metabolite Exchange Scores (MESs) to uncover key microbiome-metabolic interactions [4]. While the use of microbiome models is not novel, the application of MES to specifically investigate metabolic interactions, such as L-phenylalanine metabolism in HIV-infected individuals, provides a valuable advancement in studying microbiome–disease dynamics. With the development of advanced technology, genome-scale metabolic models (GEMs) and MICOM models that simulate microbial metabolism have the potential to explain how microbiomes interact with metabolites based on comprehensive databases that connect genes to biochemical and physiological processes [13, 14].

While numerous studies have investigated the impact of HIV infection on the gut microbiome and its associated metabolites, the specific mechanisms underlying disruptions in microbial interactions, particularly microbial cross-feeding relationships, remain poorly understood [5, 12]. Microbial cross-feeding, where one microorganism produces metabolites that are utilized by others, is crucial for maintaining a balanced gut ecosystem. Disruptions in these interactions can lead to significant metabolic and immunological changes that affect the host, but the extent to which these disruptions influence HIV pathogenesis is not well defined. In this study, we combined two available case–control 16S rRNA amplicon sequencing datasets for the gut microbiome (87 samples) that are relevant to HIV infection to investigate the intricate interactions between the gut microbiome and its metabolites in people living with HIV (PLWH). By elucidating these interactions, this study sheds light on the role of the gut microbiome in HIV pathogenesis and identifies potential therapeutic targets to mitigate the adverse effects of HIV on gut health and overall well-being.

Our research also elucidated the question of why elevated levels of phenylalanine in the bloodstream, relative to total amino acids, are observed in individuals with HIV-1 infection [15, 16]. The underlying cause of this anomaly remains unclear; however, previous evidence indicates that it is highly probable that a malfunction in the enzyme phenylalanine-4-hydroxylase (PAH) is responsible for the accumulation of phenylalanine [7–9]. In this study, our findings highlight the loss of microbial cross-feeding interactions that may lead to elevated phenylalanine levels in HIV patients. This study paves the way for future research and potential therapeutic interventions focusing on loss of microbial cross-feeding interactions among individuals with HIV. Additionally, we assessed the altered microbiomes in people living with HIV and explored the associations between HIV-related microbiome changes and factors such as disease, diet, lifestyle, and medication.

Methods and materials

Dataset identification

We conducted a search for case–control 16S studies using specific keywords ("gut microbiome," "microbiome," "HIV infection," "AIDS," "16S," "16S sequencing," "16S rRNA sequencing") in MEDLINE, Web of Science (including Cell Press, Oxford, HighWire, Science Direct, IOS Press, Springer Nature, PNAS, and Wiley), Google Scholar, and Embase. We then examined the references in the selected papers to find relevant publications. Additionally, we used artificial intelligence techniques (ResearchRabbit, Elicit, and connected papers) to detect similar papers until 20 June 2024. We first examined the titles and abstracts of publications to identify ones that might be relevant. We followed specific criteria to decide which articles to include and exclude. The criteria were as follows: (1) research that specifically investigated the association between gut microbiome and HIV infection in human samples; (2) case–control studies with comprehensive metadata; and (3) datasets that match >50% of the abundances during building community-scale metabolic models. Due to data limitations, this study only examined 16S sequencing–tested stool samples. We excluded studies that included <15 individuals with the condition under investigation. We excluded studies that specifically targeted children under the age of 5 from our findings. The dataset, which underwent quality control, consisted of 87 samples. Supplementary Data 1 includes the metadata for these samples.

16S processing

Two datasets were previously provided in tabular form, containing amplicon sequence variations (ASVs), or operational taxonomic unit abundances, while a small portion was required to be converted from raw sequences [17]. The unprocessed sequences were analyzed using the Microbiome Helper standard operating procedure in QIIME 2 version 2024.2. We conducted microbiome bioinformatics analysis using QIIME2 version 2024.2 [18]. The DADA2 method effectively removed chimeric sequences, minor mistakes, and noisy readings, producing dependable ASVs [19]. We used DADA2 via q2-dada2 to filter the raw sequence data based on the quality plot of QIIME2. The quality-control process involved applying a minimum length threshold of 80 bp and a minimum Phred score of 25 [4]. We analyzed a grand total of 438 779 reads, which included 87 samples from the 3 groups. We implemented the DADA2 algorithm for each sequencing run. All other parameters remained unchanged at their default values. After denoising, we combined the obtained feature tables to create a single "master" feature table, which includes the counts of features per sample. Each feature corresponds to a distinct variant of the 16S rRNA gene amplicon sequence. For taxonomy assignment, we used a naive Bayes classifier, which was trained on the Silva 138 database. The Silva 138 database is a widely used reference collection that includes a comprehensive set of curated 16S rRNA gene sequences from a broad range of bacterial taxa. The naive Bayes classifier was employed to assign taxonomic labels to the 16S rRNA sequences obtained in our study, enabling accurate identification of microbial species [20].

Metagenome-scale metabolic analysis

We utilized MICOM v0.35 to compute metabolic interactions among members of the microbiome community [13]. MICOM is a simulation tool that models the growth and metabolic interactions of different components of a microbiome, considering their variable abundances [13]. It has been demonstrated to accurately predict growth rates. In addition, MICOM is highly efficient in terms of computational resources, enabling the modeling of a wide range of microbial communities that can include anywhere from dozens to hundreds of species. We calculated the metabolic exchanges using MICOM's growth workflow, with a trade-off parameter of 0.5. The medium used was an average European diet, and parsimonious flux balance analysis was utilized to find the ideal growth rates and metabolic fluxes. The early CarveMe models featured a restricted range of carbon sources, leading to sluggish growth rates and numerical instability. To address this issue, we multiplied the rates of medium component transfer by a factor of 600 [4]. This was done to make it possible to calculate metabolic exchanges accurately. Afterwards, these rates were fine-tuned for the final results. We verified the bacterial growth rates projected by MICOM for all samples and found

that they were within the anticipated range, suggesting that the multiplication process did not result in implausible growth rates.

Metabolite exchange score analysis

We used the MES to understand the relationship between cross-feeding interactions and HIV infection. MES quantifies the abundance of microbial species that consume and produce a specific metabolite within a particular microbiome sample. Equation (1) describes how the MES for each metabolite is calculated using the harmonic mean of potential consumers and producers [4].

$$\mathrm{MES} = 2 \times (\mathrm{P} \times \mathrm{C}) / (\mathrm{P} + \mathrm{C})$$

P represents the number of potential producers, while C represents the number of possible consumers for specific metabolites. To identify the specific metabolites that were significantly different in cross-feeding partners between people with HIV and people who were healthy, we used the Kruskal–Wallis test. To adjust for multiple tests, we applied the Bonferroni method, dividing the target alpha of .05 by the number of tests. We conducted the studies without the presence of water or oxygen. We selected metabolites for display if they demonstrated a significant reduction in the number of cross-feeding partners and ranked among the top 10 metabolites with the highest difference in MES in HIV-positive individuals. Barplots were created and colored based on the metabolite subclass described in the Human Metabolome Database using the ggplot2 R package. Using the wordcloud package in R, we created a supplementary word cloud that included up to 100 metabolites exhibiting substantial MES changes between HIV-uninfected and infected individuals.

We applied a nested linear model to control the confounding influence of species variety on the relationships between the numbers of producers or consumers and HIV infection. We determined the rate of important metabolite transfer across microorganisms by multiplying the flux of these metabolites, measured in millimoles per hour per gram of dry weight, by the species abundances. The fluxes were subjected to a log2 transformation for both statistical analysis and graphical display [4]. We assessed the diversity of important metabolite producers and consumers, as well as the ratios of producers to consumers and their fluxes, using Kruskal–Wallis tests. We used the identified compounds expected to be released into the surrounding medium to calculate the surplus production of essential metabolites by the microbiome. We determined the net producer–consumer values for both HIV-uninfected and HIV-infected individuals. Next, we utilized the random forest (RF) model, setting the ntree parameter to 5000, to confirm the significant metabolite characteristics in the network of interactions between HIV-infected and uninfected individuals. We used the R package pROC to find the interpolated area under the receiver operating characteristic (ROC) curve (AUC) for each metabolite, taking into account their net producer–consumer relationship [21].

To determine potential species for microbiome therapy in HIV infection, we assessed the levels of important metabolites and the relative abundances of these species in both HIV-infected and healthy individuals. We calculated the fluxes of important metabolites for each microbial species by multiplying their respective fluxes by their relative abundances [4]. We calculated the aggregate of metabolite fluxes by summing all weighted fluxes within the healthy or disease groups. The variations in the combined total of important metabolites between the groups of healthy individuals and those with HIV infection indicated the primary producers and consumers of key metabolites that are linked to HIV infection.

Genome analysis

We used CarveMe v1.5 to generate genome-scale metabolic models (GEMs) across samples [22]. Archaea and bacteria were analyzed using domain-specific templates. The medium for gap filling was a typical European diet, and computations were performed using the IBM Cplex solver [23]. Next, we assessed the genetic factors underlying the production and consumption of key metabolites in the HIV-uninfected and infected individuals. In this study, we conducted a survey using a Hidden Markov Model (HMM) to identify genes involved in metabolite cycling within the microbiome. Specifically, we used HMMer v.3.3.2, a widely used tool for sequence alignment and gene identification, to search for homologous genes associated with the cycling of metabolites [24]. HMMs are highly effective for detecting conserved protein families across diverse microbial species, allowing us to identify functional domains or motifs that may be involved in key metabolic processes [25]. To ensure the accuracy of our gene identification, we applied trusted cutoff scores during the search process. These cutoff scores are thresholds designed to filter out low-confidence matches, ensuring that only the most reliable and relevant homologous genes were included in our analysis [26]. This approach helped to minimize false positives and ensured that we focused on genes with a high probability of being involved in metabolite cycling. Through this approach, we were able to pinpoint specific genes that may contribute to metabolite cycling in the microbiome, providing insights into the complex metabolic interactions in individuals with HIV. This methodology underscores the significant role that microbial genes play in regulating metabolic processes, which could inform future therapeutic strategies for modulating gut microbiome activity in HIV patients.

Statistical analysis

We measured alpha diversity using the Chao1, Observed, Abundance-based Coverage Estimator (ACE), Shannon, Simpson, and Fisher indexes, which reflect the diversity of species in each sample based on the read mapping result. We then used the Mann–Whitney to compare these measures across healthy and diseased microbiomes [27]. The R Vegan v2.6-4 package uses principal coordinates analysis (PCoA) with the Bray–Curtis distance method (10 000 permutations) to explore and visualize similarities or dissimilarities among genus levels using a PERMANOVA analysis [28]. We used the MicrobiotaProcess program to calculate the Bray–Curtis index and to visually represent all characteristics across all samples [29].

We evaluated the variations in species diversity and the correlations between the number of consumers or producers using the entire dataset, which included both healthy and diseased microbiomes. We applied a linear model (lm) in R to account for the interaction between the number of producers and consumers, as well as their respective categories (producer or consumer). We applied marginal effects to plot the association between species diversity, procedures, and consumer. We utilized Spearman correlations to assess correlations between species diversity, consumers, producers, and other related factors. Random forest classification was used to find the important microbiomes or metabolites related to HIV infections. The R package version 4.6-14 of "RandomForests" was utilized [30]. The RF classification model utilized a parameter called "ntree" with a value of 5000, indicating

the employment of 5000 trees. The "Importance" function was utilized to evaluate the predictive significance of each ASV for RF categorization. Greater values of the average decline in accuracy suggest that there are more significant variables in the RF categorization.

The taxon set enrichment analysis (TSEA) module was utilized to identify taxonomic signatures that share common functions or are associated with specific phenotypes, aiding in data interpretation and hypothesis generation. TSEA performs hypergeometric tests against a taxon set library to highlight the most significant signatures from a list of microbial features [31]. In this study, we conducted a comparative analysis of our taxon data with various taxon sets to validate our findings. These included 2179 taxon sets associated with host genetic variations, 454 sets linked to host-intrinsic factors such as diseases, 221 sets related to host-extrinsic factors like diet and lifestyle, and 293 sets associated with medication. The relationship between the studied taxa and taxon sets is tested using statistical measures, such as the raw *P*-value, Holm *P*-value, or FDR (false discovery rate), to assess the significance of the findings [31].

Results

Studied data characteristics

In order to determine the microbial cross-feeding interactions in PLWH, we obtained, processed, and re-examined the original data from a compilation of microbiome datasets. We selected studies that provided publicly accessible 16S amplicon sequencing data (in FASTQ or FASTA format) for stool samples from a minimum of 15 individuals with the condition of interest. Additionally, these studies included disease information, specifically indicating whether the individuals were cases or controls. We have identified three suitable case–control 16S datasets that meet our criteria (GenBank ID: SRP039076; GenBank ID: SRP068240; and EBI ID: ERP003611). However, the 16S data set (SRP068240) displayed a warning because the database could not match >50% of the abundances during community-scale metabolic model building. Therefore, we incorporated two additional datasets (GenBank ID: SRP039076 and EBI ID: ERP00361) for further research. Supplementary Data 1 provides information on the characteristics of these datasets, such as sample sizes, diseases, and other related factors. Supplementary Data 2, Fig. 1a, and Fig. S1 display the abundance of species along with their taxonomic categorization.

Altered microbiomes in people living with HIV

The presence of a wide range of microbial species within the gut ecosystem is often seen as an indicator of an individual's state of health [32]. We performed univariate tests on genus-level relative abundances and compared results across studies (Mann–Whitney statistic test). Microbiomes associated with HIV infection showed significant and consistent higher alpha diversity across indices [observed index (Mann–Whitney $U = 587$, P-value = .0043949), ACE index (Mann–Whitney $U = 656$, P-value = .024219)] (Fig. 1b–c and Fig. S2a–d). Beta diversity is employed to measure the disparities among the samples. This study employed two distance indices, namely, Bray–Curtis and UniFrac (weighted or unweighted), to assess the dissimilarities in community ecology. The weighted UniFrac values were subjected to a PCoA to show the beta diversity. The principal coordinates were separated effectively based on differences in ASVs (e.g. *Catenibacterium*) in HIV-infected individuals (Fig. 1d and Fig. S2). The composition of fecal microbiota differed significantly between HIV-uninfected and infected individuals ($F(df = 2) = 4.8302$, $P = .009$, $R^2 = 5.4\%$). Similar to that, there were dissimilarities in community ecology when measuring Bray–Curtis index (Fig. 1e, Bray method, P-value < .012).

Next, we identified the significant microbiome features in HIV-uninfected and infected individuals. Figure S3 illustrates the prevalence of microbiomes in these groups. *Bacteroides* (prevalence = 0.77), *Blautia* (prevalence = 0.57), and *Roseburia* (prevalence = 0.55) were found to be the most common microbiomes. In univariate models, we observed increased prevalences of *Catenibacterium*, *Dorea*, *Prevotella*, and *Erysipelotrichaceae incertae sedis* in HIV-infected individuals compared with healthy controls (EdgeR, adjusted P-value cutoff = .05) and decreased prevalences of *Anaerostipes*, *Alistipes*, *Clostridium_XI*, and *Clostridium_XlVa* in HIV-infected individuals compared with healthy controls (Fig. 2a–b and Supplementary Data 3).

The study found that HIV-infected individuals had a higher prevalence of *Catenibacterium*, *Prevotella*, and *Erysipelotrichaceae incertae sedis* compared to healthy controls after controlling for metadata available for all individuals, including study, antibiotics used in past 6 months, alcohol use, current smoking, sex, age, body mass index, education, protease inhibitor use, non-nucleoside reverse transcriptase use, and fiber consumption. Conversely, HIV-infected individuals had a lower prevalence of *Anaerostipes*, *Alistipes*, and *Bacteroides* compared to healthy controls (Fig. 2c and Table S3). We then used the RF model, which had an out-of-bag (OOB) error rate of 2.64% for the whole model, to confirm the important features of ASV abundances in the microbiome of HIV-infected and HIV-negative people (Fig. S4a). The top 15 predictors are shown in Fig. 2d. *Catenibacterium*, *Bacteroides*, *Anaerostipes*, *Erysipelotrichaceae_incertae_sedis*, and *Clostridium_XlVa* were the most important microbiomes involved in the pathogenesis of HIV infection.

Characteristics of studied metabolic exchanges

In order to analyze metabolic interactions in individuals with HIV, we employed the MICOM model to simulate the growth and metabolic exchanges within the microbiome [13]. This model accurately estimates growth rates, taking into account the varying abundances of different microbial species [4]. Figure S4b displays the growth rate of microbiomes as well as the interactions between microbiomes. Figure S5 displays the interactions between microbiomes. Interactions between species were found [PERMANOVA (pseudo-F) = 73.180, $R^2 = 0.712$, P-value = .001].

Our next step was to determine the metabolic interactions with the greatest variety of organisms that engage in cross-feeding in microbiomes by analyzing the MESs of each metabolite across all samples. Approximately 1456 metabolites in HIV-infected and uninfected individuals were found (Fig. S6). The metabolites exhibited significant variance in MESs in HIV-uninfected individuals and across all samples, as depicted in Fig. 3A, Fig. S7, and Supplementary Data 4. The metabolites with the higher average MES in HIV-uninfected individuals were proton, a 2-arylbenzofuran flavonoid (mean MES = 2.61, SD = 1.06), ammonium, a fatty acyl (2.61 ± 1.11), carbon dioxide (2.59 ± 1.12), prenol lipids such as acetate (2.47 ± 1.05), glycerol, an organonitrogen molecule (2.36 ± 1.07), amino acids [L-glutamine (2.36 ± 1.07) and L-aspartate(1−) (2.47 ± 1.06)], and succinate (2.20 ± 0.97).

Altered metabolic exchanges in people living with HIV

We conducted a comparison of MESs between individuals uninfected with HIV and those infected to determine the

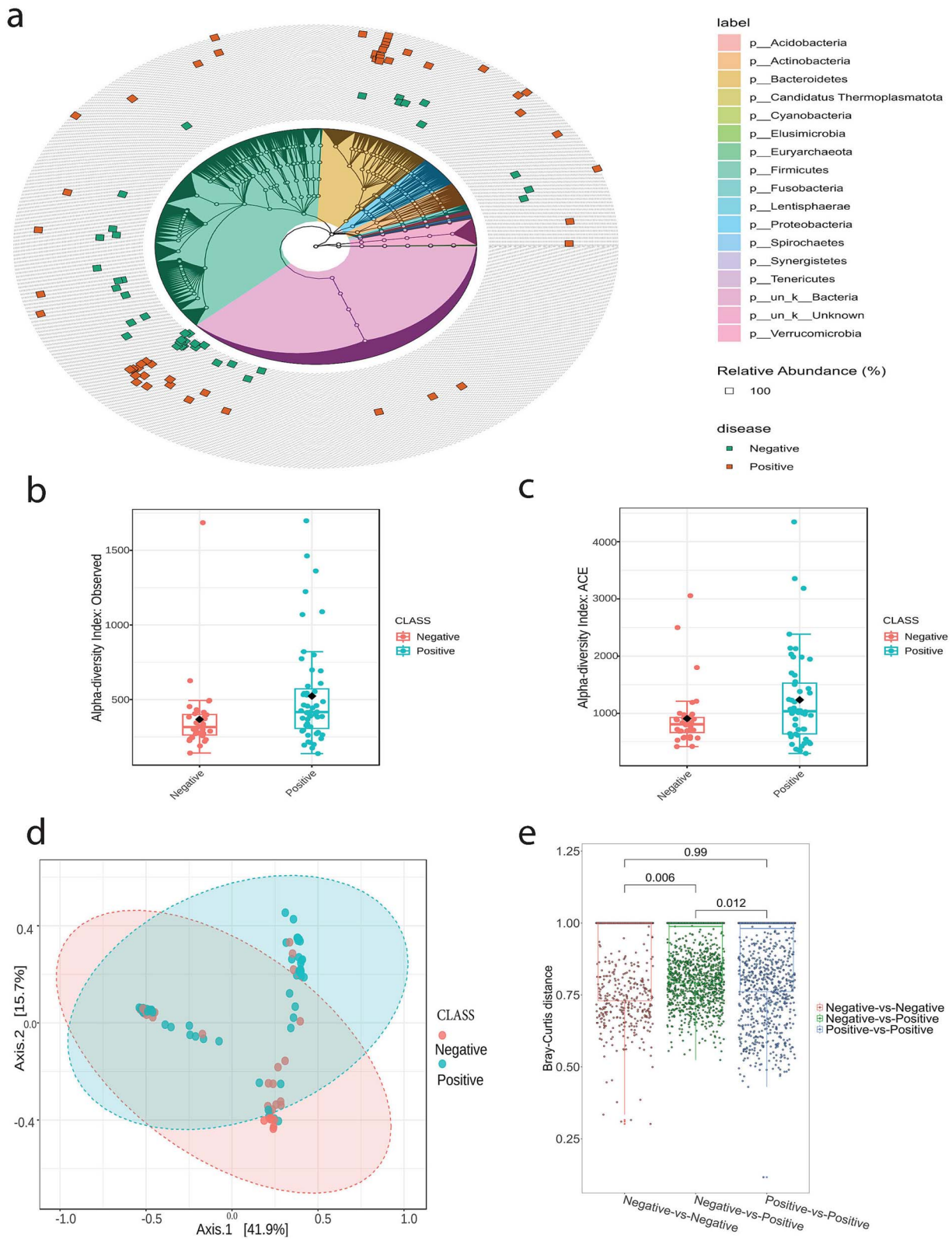

Figure 1. Microbial diversity between HIV-uninfected and HIV-infected individuals. (a) Abundance of species in HIV-uninfected and infected individuals. (b) Observed and (c) ACE index differences in HIV-uninfected and infected individuals. *P*-values were calculated using a Mann–Whitney *U* test. (d) the PCoA displays the unweighted UniFrac distances computed at the ASV (amplicon sequence variant) level, comparing HIV-uninfected and infected individuals. (e) Bray–Curtis index shows dissimilarities across all samples (Bray method, *P*-values < .012). Boxplots are displayed with the median as the center value, the box as the IQR, and the whiskers as minima and maxima.

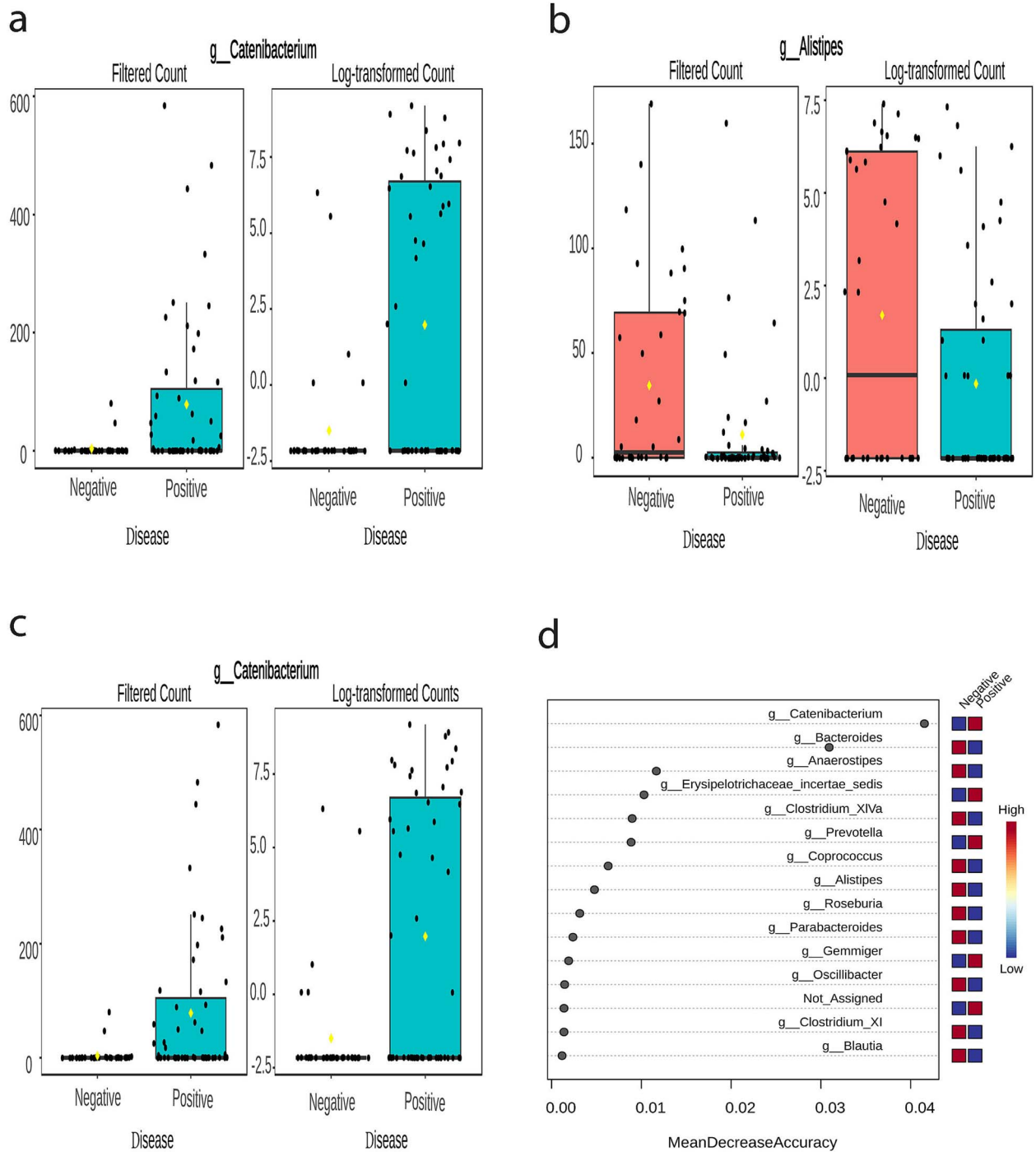

Figure 2. Composition differences between HIV-uninfected and HIV-infected individuals. (a–b) The boxplot represents the prevalence of representative microbiomes, including *Catenibacterium* and *Alistipes*. (c) The boxplot represents the prevalences of representative microbiomes, *Catenibacterium* and *Alistipes*, accounting for metadata available for all individuals, including study, antibiotics used in the past 6 months, alcohol use, current smoking, sex, age, body mass index, education, protease inhibitor use, non-nucleoside reverse transcriptase use, and fiber consumption. Boxplots including original species (filtered count) and log base 2 transform (log-transformed count) are displayed with the median as the center value, the box as the IQR, and the whiskers as minima and maxima. We obtained *P*-values for the plots using an EdgeR adjusted *P*-value cutoff of .05. (d) A random forest model determines the essential aspects of ASV abundances in the microbiome of both HIV-infected and HIV-negative individuals. The model had an OOB error rate of 2.64% for the entire dataset. The top 15 features that have the most impact on accuracy in distinguishing between HIV-uninfected and infected patients are microbiomes. Higher values of the average decrease in accuracy indicate that more important variables are present in the random forest categorization. Boxplots are displayed with the median as the center value, the box as the IQR, and the whiskers as minima and maxima.

metabolites most impacted by the loss of cross-feeding partners during disease. Essential α-amino acids (L-phenylalanine, L-leucine, and D-alanine), benzene and substituted derivatives (D-glucosamine and *N*-acetyl-D-glucosamine), and pyridoxine (the 4-methanol form of vitamin B_6) [33] had significantly higher MESs in HIV-infected individuals, whereas deoxyguanosine and urea were significantly lower MESs in HIV-infected individuals compared to HIV-uninfected individuals (Fig. S8, Fig. S9, and

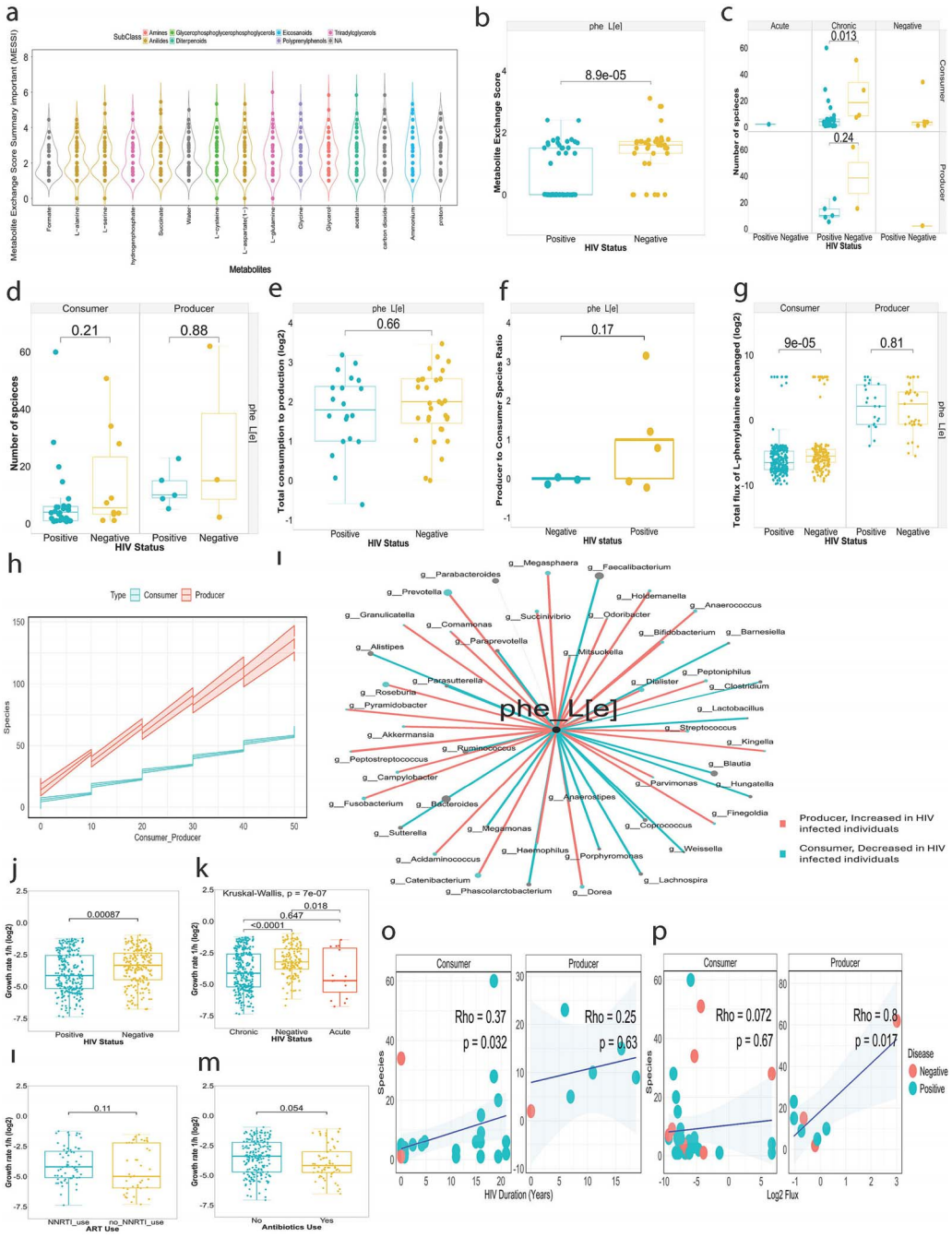

Figure 3. Metabolite exchange score and L-phenylalanine differences between HIV-uninfected and HIV-infected individuals. (a) Boxplot of metabolite exchange scores (MESs) for key metabolites in HIV-uninfected individuals, showing mean and SD. Significant metabolites include proton, a 2-arylbenzofuran flavonoid, ammonium, a fatty acyl, carbon dioxide, prenol lipids, glycerol, and various amino acids. (b) Comparison of MESs between HIV-uninfected and HIV-infected individuals. L-Phenylalanine showed statistically significant differences [Kruskal–Wallis test, the false discovery rate (FDR) P-value = .00991]. (c) Comparing the number of species capable of consuming L-phenylalanine between HIV-uninfected and HIV-infected individuals. The microbiome of HIV-uninfected individuals had a higher number of L-phenylalanine–consuming species, though the difference was not significant (Wilcoxon test, P-value = .213 for consumers and P-value = .881 for producers). (d) Comparison of the number of L-phenylalanine–consuming species between individuals with chronic HIV infection and their counterparts, showing a significant increase in the HIV-infected group (Wilcoxon test, P-value < .05). (e) Ratio of L-phenylalanine consumers to producers in HIV-uninfected versus HIV-infected individuals shows no significant variation. (f) Ratio of producers to consumers of the species L-phenylalanine in HIV-uninfected versus HIV-infected individuals shows no significant variation. (g) Total flux L-phenylalanine consumption in HIV-uninfected versus HIV-infected individuals is significantly lower in the HIV-infected group (Wilcoxon test, P-value = .0000897). (h) Marginal effects of species related to L-phenylalanine on the number of producers or consumers, indicating that the number of consumers was lower than the number of producers when considering species variety. (i) L-Phenylalanine flux, weighted by relative abundances, for key species classes (*Prevotella*, *Roseburia*, and *Catenibacterium*) in HIV-negative and HIV-positive individuals, showing that HIV patients produce more. (j) Comparison of bacterial growth rates between HIV-uninfected and HIV-infected individuals, indicating higher growth rates in the HIV-uninfected group. (k) A comparison of bacterial growth rates in HIV-uninfected versus HIV-infected individuals by HIV stage reveals that the HIV-uninfected group has higher growth rates compared to both chronic and acute stages. (l–m) A comparison of bacterial growth rates in HIV-uninfected versus HIV-infected individuals who used antiretroviral drugs (ART) and antibiotics in the past 6 months compared with their counterparts. (o–p) Correlations between HIV duration and species involved in the consumption of L-phenylalanine as well as between species involved in the production of L-phenylalanine and the flux of L-phenylalanine. Boxplots are displayed with the median as the center value, the box as the IQR, and the whiskers as minima and maxima.

Table 1. Association between species diversity and the number of consumers and producers related to L-phenylalanine in HIV-infected and uninfected individuals

Indicators	Disease		HIV stages			Consumer–producer	
	Positive β (95% confidence interval)	Negative β (95% confidence interval)	Chronic β (95% confidence interval)	Acute β (95% confidence interval)	Negative β (95% confidence interval)	Consumer β (95% confidence interval)	Producer β (95% confidence interval)
Consumer	1.14 (1.11–1.18)	1.18 (1.12–1.23)	1.13 (1.10–1.67)	1.14 (0.94–1.34)	1.22 (1.15–1.28)	1.16 (1.13–1.19)	—
Producer	2.26 (2.01–2.52)	2.39 (1.93–2.86)	2.32 (2.01–2.63)	2.07 (0.56–3.58	2.10 (1.78–2.43)	—	2.17 (1.95–2.38)

All *P*-values <.001 (detailed information is found in Table S9).

Supplementary Data 5, raw *P*-value < .0351). However, only L-phenylalanine ($C_9H_{11}NO_2$) [34] showed statistically significant differences between individuals uninfected and infected with HIV (Fig. 3b, Mann–Whitney $U = 1389.5$, FDR *P*-value = .00991).

When exploring L-phenylalanine, we observed that the number of species capable of consuming L-phenylalanine was significantly higher in individuals with chronic HIV infection compared to their counterparts (Fig. 3c, Wilcoxon test, *P*-value = .013). The microbiome of individuals uninfected with HIV had an insignificantly higher number of species capable of consuming L-phenylalanine compared to infected individuals with HIV (Fig. 3d, Mann–Whitney $U = 177.5$, *P*-value = .2133 for consumers and Mann–Whitney $U = 8.5$, *P*-value = .8808 for producers). There were no significant variations in the species ratio of L-phenylalanine consumers to producers, as well as the ratio of producers to consumers species in HIV-infected and uninfected individuals (Fig. 3e–f). Compared to their counterparts, HIV-infected patients had a lower total flux consumption of L-phenylalanine (Fig. 3g, Mann–Whitney $U = 26\ 586$, *P*-value = .0000897), but not for L-phenylalanine production (Mann–Whitney $U = 387$, *P*-value = .8115). Flux, also known as metabolic flux, refers to the rate at which molecules move through a metabolic system. The enzymes involved in a route regulate the flux [35]. Reduced enzymes involved in the metabolism of L-phenylalanine can relate to reduced flux. It is plausible to explain why L-phenylalanine MES was higher in the HIV-uninfected group.

Associations between consumers or producers and species that are capable of producing or consuming L-phenylalanine were found. Increased numbers of species increased the number of producers higher than consumers (Table 1 and Supplementary Data 6). Figure 3h shows the marginal effects of species related to L-phenylalanine on the number of producers or consumers. The number of consumers was lower than the number of producers when considering the number of species. When calculating the number of species, the number of consumers was lower than the number of producers. When considering the influence of species variety, it is clear that HIV infection had a greater impact on L-phenylalanine consumers than on L-phenylalanine producers.

Species associated with L-phenylalanine production and consumption

In order to determine which species is primarily responsible for the L-phenylalanine imbalance in individuals with HIV, we analyzed the extent to which each species contributed to the overall production or consumption of L-phenylalanine in both HIV-negative and HIV-positive individuals. We determined the L-phenylalanine flux, weighted by relative abundances, for each species. We determined the difference in total L-phenylalanine–weighted flux between HIV-uninfected and infected individuals. The classes *Prevotella*, *Roseburia*, and *Catenibacterium* exhibited a significant increase in L-phenylalanine production in HIV patients (Fig. 3I, Supplementary Data 7). Conversely, in HIV patients, the classes *Bacteroides*, *Faecalibacterium*, and *Blautia* showed the highest decrease in L-phenylalanine consumption. We next utilized our taxon data and conducted a comparative analysis with 454 taxon sets to validate our results. Our findings were in line with previous findings [36–39], which show that *Bacteroides*, *Prevotella*, *Faecalibacterium*, *Faecalibacterium*, etc. were associated with HIV infection (Supplementary Data 9, FDR < 0.0427). We also identified six genes (k141_49_21, k141_126_31, k141_104_13, k141_132_132, k141_3_2, and k141_93_61) that are related to L-phenylalanine metabolism and are involved in phenylalanine transaminase reactions with flux = 0.00573 (Fig. S10).

Bacterial growth rates associated with L-phenylalanine production and consumption

It is clear that bacterial growth rates in HIV-uninfected individuals were higher than in HIV-infected individuals (Fig. 3j, Mann–Whitney $U = 12\ 376$, *P*-value = 1.621e-05). Bacterial growth rates were significantly higher in HIV-uninfected individuals compared with acute (Fig. 3k, Kruskal–Wallis $\chi^2(1) = 5.4175$, *P*-value = .01994) and chronic stages (Kruskal–Wallis $\chi^2(1) = 27.233$, *P*-value = 1.804e-07). Bacterial growth rates were comparable in individuals who used antibiotics in the past 6 months compared with their counterparts (Fig. 3l, Mann–Whitney $U = 7942$, *P*-value = .05403) as well as in people use antiretroviral therapy (ART) drugs versus no use ART drug (Fig. 3m, Mann–Whitney $U = 1589$, *P*-value = .1143). However, several previous studies reported that the effects on the bacterial population were reduced after using ART and antibiotics (Supplementary Data 8, FDR < 0.0401). There were correlations between HIV duration and species involved in the consumption of L-phenylalanine (Fig. 3o, Rho = 0.37, *P*-value = .032), as well as between species involved in the production of L-phenylalanine and the flux of L-phenylalanine (Fig. 2p, Rho = 0.8, *P*-value = .017). Our findings suggest an increase in species capable of consuming L-phenylalanine over time, indicating a compensatory response as the disease progresses.

Correlation of species and metabolites with L-phenylalanine production and consumption in HIV-infected and HIV-uninfected individuals

Next, we identify the correlation between species, numbers of producers or consumers, and related factors [CD4 count, viral load, interferon-gamma (IFN-γ), interleukin (IL)-6, IL-1β, plasma soluble cluster of differentiation 14 (FsCD14), tumor necrosis factor alpha (TNF-α), fat, fiber, energy intake (kcal), C-reactive protein levels, plasma levels of endotoxin core immunoglobulin M (IgM; EndoCAb IgM), cholesterol, age, HIV duration, high-density

lipoprotein levels, Framingham Risk Score risk percent, low-density lipoprotein levels, etc.]. We found moderate and high correlations between the number of species and the numbers of consumers (Spearman $r = 0.93093$, P-value < .0001) and the numbers of producers (Spearman $r = 0.7002$, P-value < .0001) (Fig. 4a and Supplementary Data 10). We subsequently measured the net producer–consumer values for L-phenylalanine and other metabolites, as shown in Supplementary Data 8. We applied the prediction model to generate the ROC curve for L-phenylalanine. The AUC value of this model was 0.693 [95% confidence interval (CI), 0.591–0.790] (Fig. 4b). The average net producer–consumer value in HIV-uninfected individuals was higher than in HIV-infected individuals (Fig. 4c). The fact that HIV-uninfected individuals consumed more L-phenylalanine than their counterparts (Fig. 3g) suggests that HIV-infected individuals consume less L-phenylalanine.

After that, we used the RF model, which had an OOB error rate of 0.31% for the whole model, to confirm the important features of metabolites in the net producer–consumer relationship between HIV-positive and HIV-negative individuals (Fig. 4d). Figure 3e displays the 15 most significant predictors. (R)-Pantothenate, oxygen, siroheme, pyridoxamine, carbon dioxide, sulfate, potassium, and L-phenylalanine were the key metabolites in the net producer–consumer relationship involved in the etiology of HIV infection (Supplementary Data 11). The average of net producer–consumer values of (R)-pantothenate, an important metabolite, in HIV-uninfected individuals was higher than in HIV-infected individuals (Fig. 4f).

Association between HIV-related microbiome changes and disease, diet, lifestyle, and medication

To validate our findings, we used our taxon data to conduct a comparative analysis with different taxon sets linked to host-intrinsic factors, such as host genetic variations, diseases, diet and lifestyle, and medication. As shown in Table 2, we found that our taxon data (e.g. *Catenibacterium*, *Bacteroides*) were associated with HIV infection (total = 8, expected = 0.464, hits = 6, FDR = 6.29E-06) and acquired immunodeficiency syndrome (total = 10, expected = 0.579, hits = 8, FDR = 5.95E-08).

Dysregulation of L-phenylalanine, an essential amino acid, can contribute to various diseases and conditions, depending on whether its levels are abnormally high or low [40]. We identified several diseases associated with HIV-related microbiome changes, which could be linked to dysregulated phenylalanine, particularly through its metabolic pathways or downstream effects involving neurotransmitters, inflammation, or amino acid metabolism, such as phenylketonuria, liver cirrhosis, depression, Alzheimer's disease, hypertension, Crohn's disease, colitis, obesity, metabolic syndrome, and cardiovascular disease (all with FDR < 0.05, Table 2) [40, 41]. Additionally, we found a relationship between HIV-related microbiome changes and diet and lifestyle factors (e.g. arabinoxylan oligosaccharides, high-sucrose diet) as well as medicine (e.g. azithromycin, bismuth quadruple therapy, non-steroidal anti-inflammatory agents, and ART) (all with FDR < 0.05, Table 2). We selected the top seven microbiome taxa related to L-phenylalanine and consumer factors, including *Prevotella*, *Roseburia*, *Catenibacterium*, *Bacteroides*, *Faecalibacterium*, *Blautia*, and *Dorea*, to visualize the relationship between HIV-related microbiome changes, dysregulated phenylalanine, and diseases, diet, lifestyle, and medication. As shown in Fig. 5, there were interactions between HIV-related microbiome changes, dysregulated phenylalanine, and these factors.

Discussion

In this study, we identified L-phenylalanine as the metabolite most affected by loss of cross-feeding in HIV-infected individuals. We also find that a reduced number of species are capable of consuming L-phenylalanine during the chronic stage of HIV infection, not the acute stage. These findings partly explain the elevated levels of phenylalanine in HIV patients [15, 16].

Role of phenylalanine metabolism in HIV pathogenesis and treatment

The gut microbiota plays an important role in aromatic amino acid metabolism within the body. The host's immune response is associated with amino acids like tryptophan, phenylalanine, and tyrosine [42]. Individuals infected with HIV-1 disrupt the metabolic processes of aromatic amino acids, such as tryptophan (a precursor of serotonin), phenylalanine, and tyrosine, which are precursors of catecholamines [43]. Xiangyi Jiang *et al*. found low-molecular-weight phenylalanine derivatives to be new HIV-capsid modulators that are more effective at fighting viruses and keep the metabolism stable [44]. Phenylalanine is also an important amino acid in the process of producing catecholamines, which can alter the progression of HIV neuropathogenesis [45, 46]. HIV infections have been known to alter the ratio of phenylalanine to tyrosine [15]. An elevated phenylalanine/tyrosine ratio has been identified as a sign of immunological activation and a substitute measure for decreased tetrahydrobiopterin activity in HIV-infected individuals [7, 47]. Prior studies have reported elevated levels of phenylalanine in the bloodstream relative to total amino acids in individuals with HIV-1 infection [15, 16]. The cause of this anomaly remains unclear; however, it is highly probable that a malfunction in the enzyme phenylalanine-4-hydroxylase (PAH) is responsible for the accumulation of phenylalanine [7–9]. A recent study also discovered that the presence of HIV co-infection exacerbates COVID-19 and causes a more severe disturbance of phenylalanine metabolism [47]. The absence of cross-feeding in HIV-infected patients significantly impacts L-phenylalanine, according to our analysis. Furthermore, we observe that only a limited number of species have the ability to metabolize L-phenylalanine in the chronic phase of HIV infection, as opposed to the acute phase. The results partially elucidate the increased concentrations of phenylalanine in HIV-infected individuals [15, 16]. Remarkably, targeting phenylalanine paves the way for HIV treatment. For example, Shujing Xu *et al*. have conducted crystallographic studies and mechanistic investigations on novel phenylalanine derivatives that contain a quinazolin-4-one scaffold [48]. These derivatives have been found to be potent HIV-capsid modulators.

Impact of HIV infection on gut microbiome composition and L-phenylalanine metabolism

HIV infection is characterized by intestinal inflammation, which leads to epithelial barrier disruption and microbial translocation into the bloodstream, promoting chronic immune activation, T-cell exhaustion, and accelerating disease progression [6, 49–51]. These processes are closely associated with changes in the gut microbiota, including an increased abundance of inflammatory *Proteobacteria* and reduced microbial diversity observed in HIV patients [10, 52]. The changes in gut microbiota (e.g. *Prevotella*, *Clostridium XIVb*, *Bacteroidetes*, etc.) are strongly associated with the rise in microbial translocation and systemic inflammation in individuals with HIV infection [39, 53–55]. In this study, we found that several microbial species (e.g. *Bacteroides*, *Faecalibacterium*,

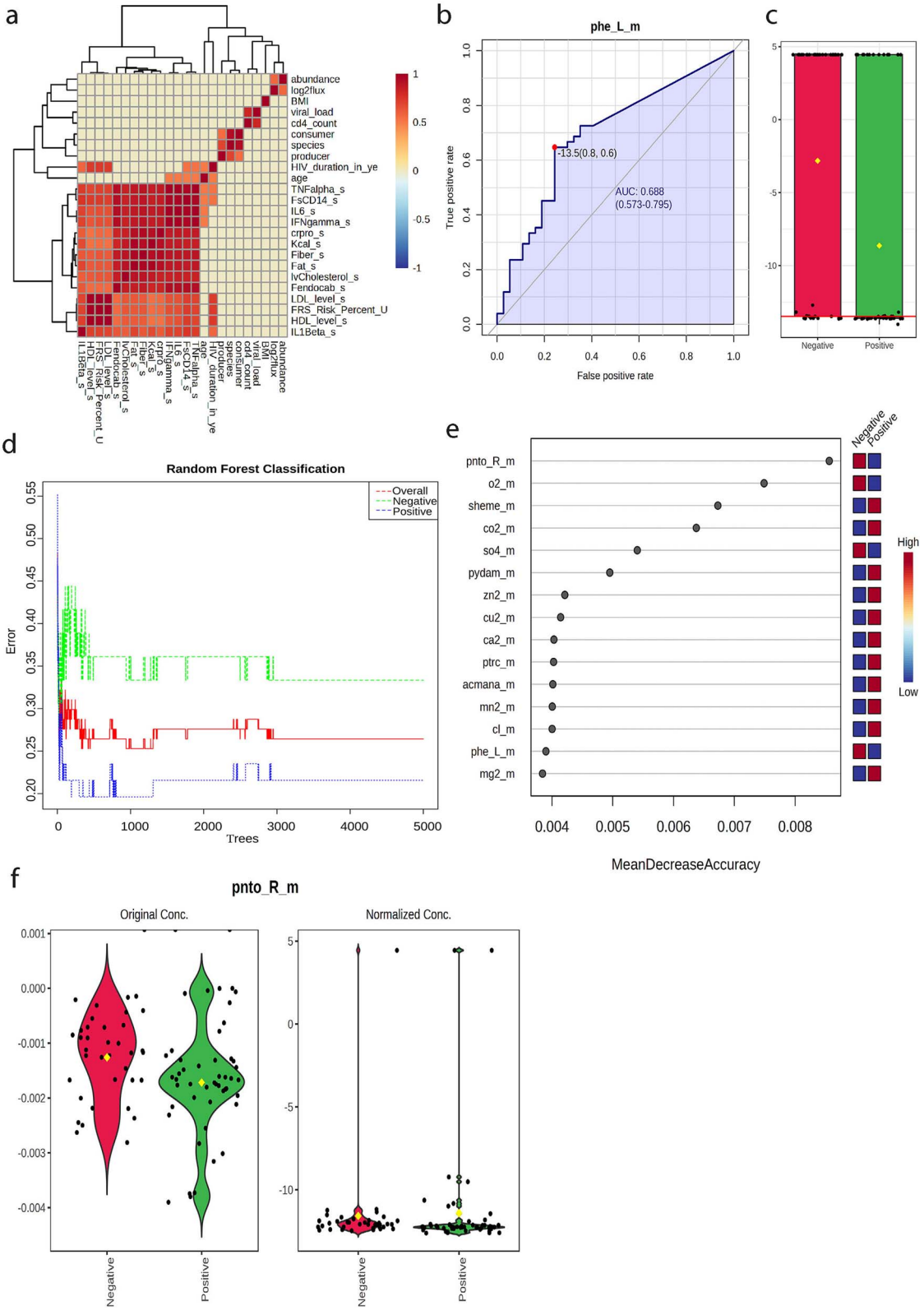

Figure 4. Correlation and net producer–consumer analysis of metabolites in HIV-uninfected and HIV-infected individuals. (a) Scatter plot showing the correlation between the number of species and the numbers of consumers (Spearman $r = 0.93093$, P-value < .001) and producers (Spearman $r = 0.7002$, P-value < .001). (b) Receiver operating characteristic (ROC) curve for L-phenylalanine using the prediction model, with an area under the curve (AUC) value of 0.693 [95% confidence interval (CI), 0.591–0.790]. (c) Comparison of average net producer–consumer values for L-phenylalanine between HIV-uninfected and HIV-infected individuals, showing higher values in the HIV-uninfected group. (d) Random forest (RF) model confirmation of significant metabolite features with an OOB error rate of 0.31%. (e) Top 15 significant predictors of HIV status based on the RF model, identifying key metabolites such as (R)-pantothenate, oxygen, siroheme, pyridoxamine, carbon dioxide, sulfate, potassium, and L-phenylalanine in the net producer–consumer relationship involved in HIV infection etiology. (f) Comparison of average net producer–consumer values of (R)-pantothenate between HIV-uninfected and HIV-infected individuals, showing higher values in the HIV-uninfected group. Boxplots including original species (filtered count) and log base 2 transform (log-transformed count) are displayed with the median as the center value, the box as the IQR, and the whiskers as minima and maxima.

Table 2. Associations between HIV-related microbiome changes and disease, diet, lifestyle, and medication

Indicators	Microbiome	Microbiome change	Total	Expected	Hits	Raw P	Holm P	FDR
Disease								
HIV infection[a]	**Bacteroides**; Bacteroidetes; **Faecalibacterium**; Lachnospira; **Parabacteroides**; **Phascolarctobacterium**; **Roseburia**; **Sutterella**	Decrease	8	0.464	6	8.60E-07	0.00034	6.29E-06
Acquired immunodeficiency syndrome	**Butyricicoccus**; **Catenibacterium**; **Dorea; Enterobacter**; Enterococcus; Erysipelotrichaceae incertae sedis; **Faecalibacterium**; **Megamonas**; **Phascolarctobacterium**; **Prevotella**	Increase	10	0.579	8	4.20E-09	1.77E-06	5.95E-08
Phenylketonurias	Clostridiaceae; **Coprococcus**; **Dorea**; Erysipelotrichaceae; Lachnospira; Lachnospiraceae; **Odoribacter**; **Ruminococcus**; **Veillonella**	Decrease	9	0.522	5	6.32E-05	0.0221	0.000266
Liver cirrhosis	**Veillonella**; Enterobacteriaceae; Lactobacillaceae; **Porphyromonas**; Staphylococcaceae; **Actinobacillus**; *Anaeroglobus geminatus*; **Enterobacter**; Gammaproteobacteria; *Haemophilus parainfluenzae*; Klebsiella; *Megasphaera micronuciformis*; Neisseriaceae; *Paraprevotella clara*; Sphingomonadaceae; Streptococcus; *Escherichia coli*; Firmicutes; **Akkermansia; Alloprevotella**; **Citrobacter**; Escherichia; **Haemophilus**; **Lactobacillus**; Micrococcus; Pediococcus; Weissella; Enterococcus; **Bifidobacterium**; Pasteurellaceae; Bacteroidetes; **Faecalibacterium**; Streptococcaceae; Veillonellaceae; Intestinibacter; Lachnoclostridium; Lachnospiraceae Ucg-010; **Odoribacter**; **Parabacteroides**; **Paraprevotella**; **Eubacterium**; **Ruminococcus**; *Pediococcus pentosaceus* Li05	Increase	43	2.49	17	3.84E-11	1.67E-08	8.31E-10
Depressive disorder, major	Bacteroidetes; Agathobacter; **Bifidobacterium**; **Blautia; Butyricicoccus**; Coprococcus 3; Coriobacteriales; **Dorea; Faecalibacterium**; Fusicatenibacter; Lachnospiraceae ND3007 group; **Roseburia**; Ruminococcaceae UCG-013; Ruminococcus 1; **Subdoligranulum**	Decrease	15	0.869	7	8.13E-06	0.00309	4.92E-05
Alzheimer's disease	**Blautia; Bacteroides; Alistipes; Phascolarctobacterium; Bilophila; Gemella**	Increase	6	0.348	6	3.38E-08	1.41E-05	3.84E-07
Autism	**Selenomonas; Prevotella; Fusobacterium**; TM7_[G-1]; **Treponema; Tannerella**; Veillonellaceae_[G-1]; **Alloprevotella; Olsenella; Dialister; Oribacterium; Peptococcus; Parvimonas; Peptostreptococcus; Atopobium**; Peptostreptococcaceae_[XI][G-9]	Decrease	16	0.927	13	2.21E-14	9.85E-12	1.11E-12
Hypertension	Lachnospiraceae; **Adlercreutzia**; Aeromicrobium; Akkermansia; Anaerofustis; Arcobacter; **Bifidobacterium**; **Bilophila**; Brevibacterium; Buchnera; **Dorea; Facklamia; Faecalibacterium**; Fusobacteria; **Granulicatella**; Jeotgalicoccus; **Lactobacillus**; **Lactococcus**; Methylibim; Microbispora; Modestobacter; **Odoribacter**; **Parabacteroides; Paraprevotella; Peptoniphilus; Pseudomonas**; Rathayibacter; RC4-4; Rhodococcus; **Rikenella; Ruminococcus**; Selenomonas; Sphingomonadaceae; Staphylococcus; Steroidobacter; **Sutterella**; *Tannerella forsythia*; **Veillonella**; Weissella; Xylanimicrobium	Increase	40	2.32	19	3.94E-14	1.75E-11	1.79E-12
Crohn disease	Fungus; **Akkermansia; Alistipes; Coprococcus; Dorea; Eubacterium; Prevotella; Roseburia; Ruminococcus; Veillonella; Collinsella; Enterorhabdus**; Gordonibacter; Bacteroidetes; **Anaerostipes; Blautia; Faecalibacterium**; Lachnospira; **Odoribacter; Bifidobacterium; Streptococcus**; *Bacteroides xylanolyticus*; *Bifidobacterium catenulatum*; Blautia ruminococcus; *Clostridium perfringens*; *Clostridium disporicum*; Intestinibacter bartlettii; *Roseburia cecicola*; *Streptococcus salivarius*; Clostridium; Firmicutes; **Desulfovibrio; Barnesiella; Parabacteroides**; Porphyromonadaceae; Cyanobacteria	Decrease	36	2.09	20	1.40E-16	6.30E-14	1.27E-14
Colitis, ulcerative	Clostridia; Clostridium; Coriobacteriia; Firmicutes; Lentisphaerae; Verrucomicrobiae; **Bifidobacterium; Lactobacillus**; *Faecalibacterium prausnitzii*; **Alistipes; Anaerotruncus; Collinsella**; Coprobacter; Flavonifractor; **Megasphaera; Odoribacter**; Oscillospira; **Paraprevotella; Parasutterella; Subdoligranulum**; Thalassospira; *Bilophila wadsworthia*; Eubacteriales; *Eubacterium rectale*; 02d06; Bacteroidetes; **Butyricimonas**; **Desulfovibrio; Holdemania**; Lachnobacterium; **Megamonas; Mitsuokella; Oxalobacter; Prevotella**; Pyramidobacter; Synergistes; **Victivallis**	Decrease	37	2.14	18	1.16E-13	5.13E-11	4.05E-12

(continued)

Table 2. Continued

Indicators	Microbiome	Microbiome change	Total	Expected	Hits	Raw *P*	Holm *P*	FDR
Obesity	Acidobacteria; Firmicutes; Proteobacteria; **Akkermansia; Blautia**; **Coprococcus**; Lachnospiraceae; **Moryella**; Peptococcaceae; **Roseburia; Ruminococcus**; Helicobacter; Mucispirillum; **Butyricicoccus**; *C. perfringens*; Bacillus; Clostridia; **Prevotella; Treponema; Bifidobacterium**; **Lactobacillus; Parabacteroides**; *Akkermansia muciniphila*; Deferribacteres; **Staphylococcus**; Desulfovibrionaceae; Aliihoeflea; Christensenellaceae R-7 Group; **Desulfovibrio; Lactococcus**; Bacteroidetes; Deferribacteria; Erysipelotrichaceae; Helicobacteraceae; Ruminococcaceae; Actinobacteria; Erysipelotrichi; Gammaproteobacteria; **Citrobacter; Cronobacter**; Enterobacteriaceae; *E. coli*; Klebsiella; microbiota from high-fat diet–raised mice; Bifidobacteria; Af12; Lactobacillaceae; **Alistipes; Anaerotruncus; Dorea; Anaeroplasma; Bacteroides**; Clostridiales; microbiota from Western diet mice; Oscillospira; S24-7; Clostridium; Epsilonproteobacteria; Bifidobacteriaceae; Coriobacteriaceae; Escherichia; **Streptococcus**; Tenericutes; Sporosarcina	Increase	64	3.71	23	1.02E-13	4.51E-11	4.05E-12
Metabolic syndrome	**Akkermansia; Bifidobacterium; Lactobacillus**; Methanobrevibacter; **Odoribacter; Sutterella**; *Bacteroides fragilis*; Betaproteobacteria; **Anaerostipes**; Bacteroidaceae; **Blautia; Collinsella**; **Coprobacillus**; Lachnospiraceae; Oscillospira; Ruminococcaceae; **Ruminococcus**; Tissierellaceae; Bacteroidetes; Erysipelotrichaceae; **Holdemania**; *B. wadsworthia*; **Desulfovibrio**; Enterococcus; Clostridiaceae; Bifidobacteriaceae; Enterococcaceae; **Granulicatella**; **Coprococcus**; *Lactobacillus rhamnosus* NCIMB 6375; **Bacteroides**; Escherichia; Fusobacteria; **Proteobacteria**; Allobaculum; Porphyromonas; Candidatus portiera; Clostridium; Dickeya; SMB53; **Succinivibrio**; **Faecalibacterium**; Lachnospira; Caulobacteraceae; Firmicutes	Increase	45	2.61	18	7.60E-12	3.32E-09	1.92E-10
Cardiovascular diseases	*B. fragilis*; Betaproteobacteria; **Bifidobacterium**; Burkholderiales; Aggregatibacter; Anaerovibrio; Bacteroidetes; **Dorea**; Lachnospiraceae; **Phascolarctobacterium**; **Prevotella**; Prevotellaceae; RC4-4; **Sutterella**; YS-2; TMAO-producing microbiota; Oscillospira; **Turicibacter**; urolithin-producing microbiota; **Odoribacter**	Decrease	20	1.16	7	7.67E-05	0.0265	0.000314
Diet and lifestyle								
Arabinoxylan oligosaccharides; obesity	**Anaerostipes; Bifidobacterium; Blautia; Coprococcus; Dorea; Eubacterium; Faecalibacterium**; Fusicatenibacter; **Roseburia; Ruminococcus**	Increase	10	2.21	9	8.30E-06	0.00183	0.00183
High-sucrose diet	**Acinetobacter; Alistipes; Anaerotruncus; Bacteroides; Blautia; Dorea; Oscillibacter**; Proteobacteria	Increase	8	1.77	7	0.000149	0.0327	0.0164
Medication								
Azithromycin; health	Achromobacter; **Actinobacillus; Actinomyces**; alkaliphilus; Anaerobranca; Anaerovibrio; Arcanobacterium; bacillus; Borrelia; Bulleidia; Caloramator; **Campylobacter**; Candidatus Blochmannia; Candidatus Glomeribacter; **Catenibacterium**; **Collinsella**; Cyanobacterium; Desulfonauticus; Desulfosarcina; **Desulfovibrio; Elusimicrobium**; **Fusobacterium**; **Gemella**; Geobacter; **Granulicatella**; **Haemophilus**; Helicobacter; **Lactobacillus**; Leptospira; Mannheimia; **Megasphaera**; **Mitsuokella**; **Mogibacterium**; **Moryella**; **Negativicoccus**; Olivibacter; Paenibacillus; Paucibacter; **Peptococcus; Peptoniphilus; Peptostreptococcus; Phascolarctobacterium**; Polaribacter; **Porphyromonas; Rothia**; Schlegelella; **Selenomonas**; Shewanella; Sphingobacterium; **Succinivibrio; Sutterella**; Thermicanus; Thermodesulfovibrio	Decrease	53	9.27	26	3.35E-08	1.04E-05	1.04E-05
Bismuth quadruple therapy; gastritis	**Akkermansia; Bacteroides; Bifidobacterium; Butyricimonas; Collinsella**; Eggerthella; **Odoribacter; Paraprevotella; Prevotella**; Wautersiella	Decrease	10	1.75	8	2.38E-05	0.0074	0.00371
Anti-inflammatory agents, non-steroidal (indomethacin, ibuprofen, ketoprofen, diclofenac, piroxicam, celecoxib, nimesulid, and aspirin); aged	**Collinsella; Coprobacillus; Dialister; Collinsella; Lactobacillus**	Decrease	5	0.874	5	0.000153	0.0475	0.0119
Antiretroviral therapy, highly active; HIV infections	**Anaerococcus; Campylobacter; Finegoldia; Peptoniphilus; Prevotella**	Increase	5	0.874	5	0.000153	0.0475	0.0119

Microbiome hits are highlighted in bold. Expected: the number of taxa that would be expected to be found by chance based on the distribution in the dataset (0.464 in this case). Expected serves as a baseline to compare the actual hits. If the actual hits (6 in this case) greatly exceed the expected value (0.464), it suggests that the observed association is unlikely due to chance and may be biologically significant. This relationship is tested using statistical measures, such as the raw *P*-value, Holm *P*-value, or FDR (false discovery rate), to confirm the significance of the finding. [a]Total: the total number of taxa associated with the condition (e.g. HIV infection) in the analysis (8 in this case); Hits: The actual number of those taxa found in this dataset (6 in this case).

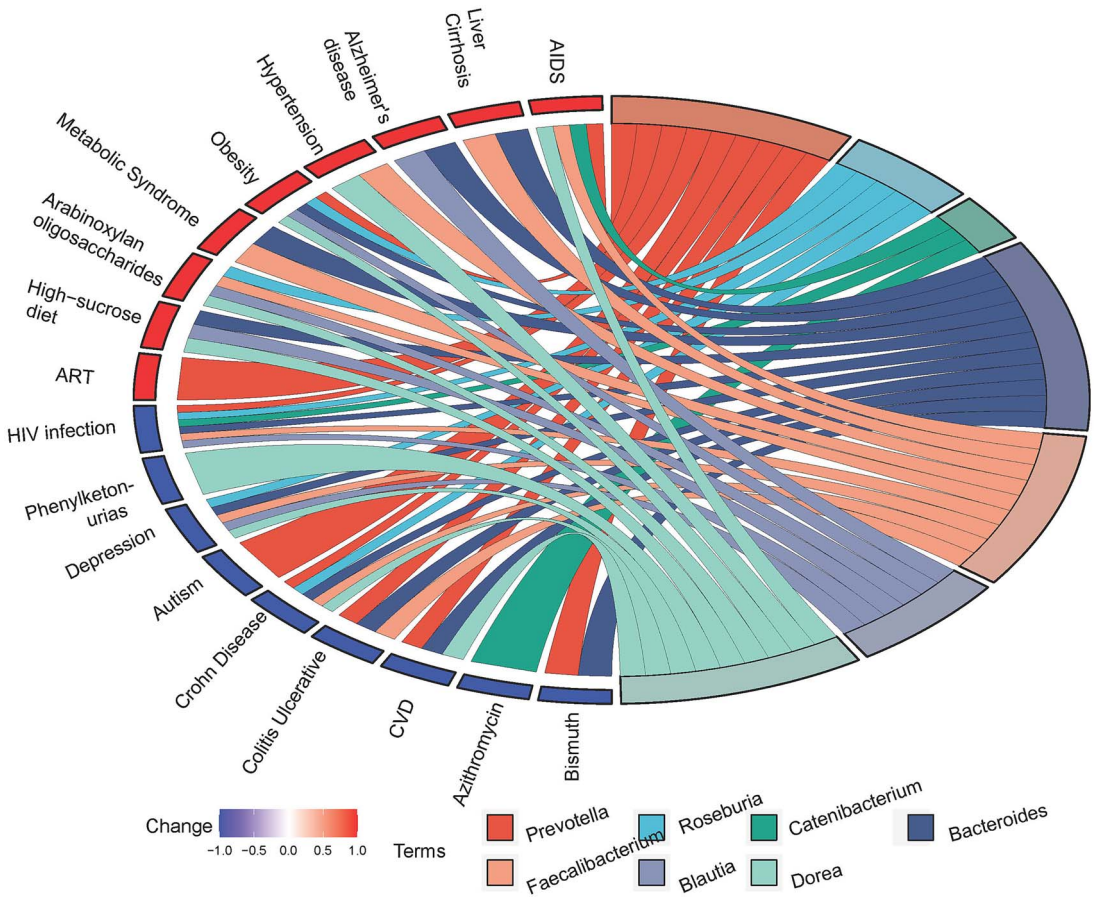

Figure 5. Interactions between HIV-related microbiome changes, dysregulated L-phenylalanine, and associated diseases, diet, lifestyle, and medications. This figure visualizes the relationships between HIV-related microbiome changes, dysregulated L-phenylalanine levels, and various factors such as diseases (e.g. phenylketonuria, liver cirrhosis, depression, Alzheimer's disease, hypertension, Crohn's disease, colitis, obesity, metabolic syndrome, cardiovascular disease), diet and lifestyle factors (e.g. arabinoxylan oligosaccharides, high-sucrose diet), and medications (e.g. azithromycin, bismuth quadruple therapy, non-steroidal anti-inflammatory agents, and antiretroviral therapy). The top seven microbiome taxa linked to L-phenylalanine dysregulation are highlighted: *Prevotella*, *Roseburia*, *Catenibacterium*, *Bacteroides*, *Faecalibacterium*, *Blautia*, and *Dorea*. the taxon set enrichment analysis (TSEA) module was used to identify taxonomic signatures associated with specific phenotypes, facilitating data interpretation and hypothesis generation. The relationship between the studied taxa and taxon sets is tested using statistical measures, such as raw *P*-values, Holm *P*-values, or the false discovery rate (FDR), to assess the significance of the findings. All data points are associated with an FDR < 0.05, as indicated in Table 2.

Blautia, *Parabacteroides*, *Alistipes*, *Ruminococcus*, *Phascolarctobacterium*, *Coprococcus*, *Sutterella*, and *Lachnospira*) are capable of consuming phenylalanine, which is significantly reduced in HIV-infected individuals compared to their counterparts (Table S7). Several microbiomes (*Prevotella*, *Roseburia*, *Catenibacterium*, *Dialister*, *Megasphaera*, *Dorea*, *Fusobacterium*, *Acidaminococcus*, *Succinivibrio*, and *Anaerococcus*) are capable of producing phenylalanine, which significantly increased in HIV-infected individuals compared to their counterparts. These microbiomes have been found to be associated with the pathogenesis of HIV infection [36–39]. Although there is no statistically significant difference between the occurrence of species (Mann–Whitney $U = 172.5$, P-value = .05182) in the microbiome capable of producer and consumer, there is a significant difference in the weighted flux sum in these groups (Mann–Whitney $U = 151$, P-value = .01516). There was a notable disparity in the fecal microbiota makeup between those who were uninfected with HIV and those who were infected. The microbiomes associated with HIV infection consistently exhibited higher alpha diversity, as indicated by the Observed index and ACE index. Individuals with HIV in the chronic stage, on the other hand, may experience low species richness, which can result in the accumulation of phenylalanine due to consumption. Perhaps, during the acute stage, certain species seek to be self-sufficient in consuming these metabolites as a decompensatory measure [4].

Impact of microbial cross-feeding and L-phenylalanine metabolism on HIV pathogenesis and treatment outcomes

The observed changes in microbial cross-feeding and L-phenylalanine metabolism in individuals with HIV may be driven by several biological mechanisms that affect disease progression and treatment outcomes. HIV infection disrupts the gut microbiome, leading to the depletion of beneficial species like *Faecalibacterium*, which are involved in butyrate production [11]. This loss impairs microbial cross-feeding and L-phenylalanine metabolism, potentially contributing to elevated phenylalanine levels and gut dysfunction. In addition, HIV-induced chronic inflammation alters the gut environment, promoting species such as *Prevotella* and *Roseburia*, which may exacerbate metabolic imbalances [11]. This inflammatory response likely elevates phenylalanine levels, further affecting immune function and disease progression [56]. Disruptions in microbial cross-feeding lead to shifts in the host's metabolic profile, influencing immune modulation and potentially reducing the effectiveness of ART [57]. Dysregulated L-phenylalanine metabolism, linked to cognitive

decline and immune dysfunction, may impair ART efficacy and contribute to persistent viral replication [43, 56, 58]. In line with our findings, a study of 398 participants identified a distinct gut microbiome in people with HIV and impaired activities of daily living, enriched in *Bacteroides*, previously linked to cognitive decline [59, 60]. Another study of 85 antiretroviral-naïve HIV-infected subjects found lower abundances of *Faecalibacterium*, *Catenibacterium*, and *Ruminococcaceae* in those with HIV-associated neurological diseases (HAND) compared to those without HAND [5]. Our analysis revealed significant associations between HIV-related microbiome changes and host-intrinsic factors such as genetic variations, diseases, diet, lifestyle, and medication. Key species (e.g. *Catenibacterium* and *Bacteroides*) were linked to HIV infection and AIDS, offering new insights into the microbiome's role in HIV pathogenesis. Dysregulated L-phenylalanine levels were associated with several conditions, including depression, Alzheimer's, and cardiovascular diseases, highlighting the impact of microbiome shifts on metabolic and neurological processes in HIV-infected individuals. Additionally, we identified interactions between microbiome changes and lifestyle factors (e.g. diet and medications), suggesting potential targets for therapeutic interventions. By visualizing the top microbiome taxa related to L-phenylalanine, including *Prevotella*, *Roseburia*, and *Faecalibacterium*, we further clarified the microbial role in phenylalanine metabolism. These findings underscore the importance of the HIV-associated microbiome in disease progression and suggest that microbiome modulation could improve clinical management of HIV-related health issues. In conclusion, microbial cross-feeding and L-phenylalanine metabolism are crucial in HIV pathogenesis, and their disruption contributes to chronic inflammation, immune dysfunction, and potentially impaired treatment outcomes. Future studies should explore these mechanisms to develop more targeted therapeutic strategies.

Model performance and insights into microbial interactions in HIV infection

We used the prediction model to create the ROC curve for L-phenylalanine. The AUC value of the model was 0.693. While this value may appear relatively modest, it is important to note that it indicates the model performs better than random chance (which would yield an AUC of 0.5). Given the complexity and heterogeneity of microbiome data, particularly in the context of HIV infection, an AUC value of 0.693 can be considered a reasonable result. The goal of this study was not to achieve perfect classification, but rather to identify significant patterns and trends associated with microbial cross-feeding interactions in individuals living with HIV. Several factors contribute to the model's performance, including the inherent noise and variability in microbiome data [61]. Microbial populations vary substantially across individuals, and the relatively small sample size may have influenced the model's ability to achieve higher classification accuracy. Moreover, microbiome data are often high-dimensional, and such datasets tend to pose challenges for any classifier in terms of overfitting and generalization [62]. We selected the RF classifier for its robustness and ability to handle high-dimensional data without overfitting. Random forests are well suited for complex, nonlinear relationships and provide important insights into feature importance. Despite the possibility that other classifiers, such as gradient boosting machines or support vector machines, could potentially improve the AUC, the RF model was deemed the most appropriate for this study's dataset. While the AUC value could be improved, it is important to emphasize that the current model has provided valuable insights into the microbial interactions and metabolic changes associated with HIV infection. Future work could explore alternative classifiers or optimize the current model through additional data and hyperparameter tuning to improve performance further.

Limitations

This analysis is the first research effort to detect the loss of microbial cross-feeding interactions among individuals with HIV. However, there are several limitations that should be considered. The sample size used in this study (87 samples) is relatively modest, which is a common challenge in microbiome studies of HIV, where cohort availability, data quality, and specific inclusion criteria may restrict the number of samples. While this sample size provides valuable insights into the microbiome-metabolic interactions in HIV-infected individuals, future studies with larger cohorts would enhance the robustness and generalizability of the findings, especially when examining more granular aspects of microbial interactions and their implications on health outcomes. Additionally, one important dataset, the 16S rRNA data set (SRP068240), was excluded from the analysis due to its failure to match >50% of the abundances during the construction of community-scale metabolic models. This exclusion may limit the comprehensiveness of the analysis, and future investigations should consider incorporating additional datasets to strengthen the robustness of the findings and extend the exploration of microbial interactions in HIV infection. While the present study provides valuable insights into the loss of microbial cross-feeding relationships in HIV infection, further research with more diverse and larger cohorts is needed to validate and expand upon these findings. Future studies should also explore different microbiome profiling techniques, such as shotgun metagenomics, to provide a more comprehensive view of microbial metabolism and its influence on HIV pathology.

In conclusion, we found that only a limited number of species can metabolize L-phenylalanine during the chronic phase of HIV infection, not the acute phase. In chronic HIV infection, the loss of cross-feeding has a significant impact on the metabolite L-phenylalanine. Currently, many theories also believe that the elevated phenylalanine levels observed in HIV patients are attributed to the deficiency of the enzyme PAH, which is responsible for the buildup of phenylalanine [7–9]. We also found a particular microbiome that is capable of producing or consuming phenylalanine. These results pave the way for future research that can apply our findings to gain a better understanding of the ecology of these intricate gut communities and discover more effective approaches for treating HIV. Future translational research should focus on therapeutic strategies targeting microbial classes such as *Prevotella*, *Roseburia*, and *Catenibacterium*, which exhibited a significant increase in L-phenylalanine production in HIV patients. Conversely, therapeutic efforts could also aim to enhance the functionality of classes like *Bacteroides*, *Faecalibacterium*, and *Blautia*, which showed the highest decrease in L-phenylalanine consumption in HIV patients. Modulating these microbial communities could potentially restore metabolic balance and improve gut health in individuals living with HIV. Although previous studies have demonstrated the impact of gut microbiota on HIV pathogenesis, our research is one of the first to integrate microbial cross-feeding interactions and their direct influence on phenylalanine metabolism in the chronic stage of HIV infection [12]. These results open the door for future translational research aimed at modulating the gut microbiome to improve metabolic outcomes and overall health in HIV patients.

Key Points

- In HIV patients, L-phenylalanine had a lower MES.
- The flux of L-phenylalanine consumption was significantly lower in HIV-infected individuals.
- A decrease in the number of species that consume L-phenylalanine during the chronic stage was observed.
- *Prevotella*, *Roseburia*, and *Catenibacterium* contributed to an increase in L-phenylalanine production in HIV patients.
- *Bacteroides*, *Faecalibacterium*, and *Blautia* contributed to a decrease in L-phenylalanine consumption in HIV patients.

Acknowledgements

Technical assistance from Dr Chrys Perdios is greatly appreciated. This work was conducted at the Tulane National Primate Research Center (TNPRC RRID: SCR_008167) and supported by the TNPRC P51 Base Grant (P51OD011104) from the National Institutes of Health.

Author contributions

Hai Duc Nguyen (Writing—review & editing, Writing—original draft, Visualization, Validation, Software, Resources, Methodology, Investigation, Formal analysis, Data curation, Conceptualization) and Woong-Ki Kim (Supervision, Project administration, Funding acquisition, Writing—review & editing).

Supplementary data

Supplementary data is available at *Briefings in Bioinformatics* online.

Conflict of interest: None declared.

Funding

This work was conducted at the Tulane National Primate Research Center (TNPRC RRID: SCR_008167) and supported by the TNPRC P51 Base Grant (P51OD011104) from the National Institutes of Health.

Data availability

The raw sequencing data for each research project can be obtained by following the instructions provided in Supplementary Data 1 (GenBank ID: SRP039076 and EBI ID: ERP003611). All further pertinent data that substantiate the conclusions of the research can be found in this publication and its Supplementary Information files or can be obtained from the corresponding author upon request.

References

1. Wu H-J, Wu E. The role of gut microbiota in immune homeostasis and autoimmunity. *Gut Microbes* 2012;**3**:4–14. https://doi.org/10.4161/gmic.19320
2. Hou K, Wu Z-X, Chen X-Y. *et al.* Microbiota in health and diseases. *Signal Transduct Target Ther* 2022;**7**:1–28.
3. Culp EJ, Goodman AL. Cross-feeding in the gut microbiome: ecology and mechanisms. *Cell Host Microbe* 2023;**31**:485–99. https://doi.org/10.1016/j.chom.2023.03.016
4. Marcelino VR, Welsh C, Diener C. *et al.* Disease-specific loss of microbial cross-feeding interactions in the human gut. *Nat Commun* 2023;**14**:6546. https://doi.org/10.1038/s41467-023-42112-w
5. Zhang Y, Xie Z, Zhou J. *et al.* The altered metabolites contributed by dysbiosis of gut microbiota are associated with microbial translocation and immune activation during HIV infection. *Front Immunol* 2023;**13**:1020822. https://doi.org/10.3389/fimmu.2022.1020822
6. Zevin AS, McKinnon L, Burgener A. *et al.* Microbial translocation and microbiome dysbiosis in HIV-associated immune activation. *Curr Opin HIV AIDS* 2016;**11**:182–90. https://doi.org/10.1097/COH.0000000000000234
7. Shintaku H. Disorders of tetrahydrobiopterin metabolism and their treatment. *Curr Drug Metab* 2002;**3**:123–31. https://doi.org/10.2174/1389200024605145
8. Anderson DN, Wilkinson AM, Abou-Saleh MT. *et al.* Recovery from depression after electroconvulsive therapy is accompanied by evidence of increased tetrahydrobiopterin-dependent hydroxylation. *Acta Psychiatr Scand* 1994;**90**:10–3. https://doi.org/10.1111/j.1600-0447.1994.tb01547.x
9. Neurauter G, Schrocksnadel K, Scholl-Burgi S. *et al.* Chronic immune stimulation correlates with reduced phenylalanine turnover. *Curr Drug Metab* 2008;**9**:622–7. https://doi.org/10.2174/138920008785821738
10. Vujkovic-Cvijin I, Somsouk M. HIV and the gut microbiota: composition, consequences, and avenues for amelioration. *Curr HIV/AIDS Rep* 2019;**16**:204–13. https://doi.org/10.1007/s11904-019-00441-w
11. Dillon SM, Kibbie J, Lee EJ. *et al.* Low abundance of colonic butyrate-producing bacteria in HIV infection is associated with microbial translocation and immune activation. *AIDS Lond Engl* 2017;**31**:511–21. https://doi.org/10.1097/QAD.0000000000001366
12. Nganou-Makamdop K, Talla A, Sharma AA. *et al.* Translocated microbiome composition determines immunological outcome in treated HIV infection. *Cell* 2021;**184**:3899–3914.e16. https://doi.org/10.1016/j.cell.2021.05.023
13. Diener C, Gibbons SM, Resendis-Antonio O. MICOM: metagenome-scale modeling to infer metabolic interactions in the gut microbiota. *mSystems* 2020;**5**:e00606–19. https://doi.org/10.1128/msystems.00606-19
14. Heinken A, Hertel J, Acharya G. *et al.* Genome-scale metabolic reconstruction of 7,302 human microorganisms for personalized medicine. *Nat Biotechnol* 2023;**41**:1320–31. https://doi.org/10.1038/s41587-022-01628-0
15. Zangerle R, Kurz K, Neurauter G. *et al.* Increased blood phenylalanine to tyrosine ratio in HIV-1 infection and correction following effective antiretroviral therapy. *Brain Behav Immun* 2010;**24**:403–8. https://doi.org/10.1016/j.bbi.2009.11.004
16. Ollenschläger G, Jansen S, Schindler J. *et al.* Plasma amino acid pattern of patients with HIV infection. *Clin Chem* 1988;**34**:1787–9. https://doi.org/10.1093/clinchem/34.9.1781
17. Duvallet C, Gibbons SM, Gurry T. *et al.* Meta-analysis of gut microbiome studies identifies disease-specific and shared responses. *Nat Commun* 2017;**8**:1784. https://doi.org/10.1038/s41467-017-01973-8
18. QIIME 2 user documentation—QIIME 2 2024.2.0 documentation.
19. Callahan BJ, McMurdie PJ, Rosen MJ. *et al.* DADA2: high resolution sample inference from Illumina amplicon data. *Nat Methods* 2016;**13**:581–3. https://doi.org/10.1038/nmeth.3869
20. QIIME 2 Resources.

21. Robin X, Turck N, Hainard A. *et al.* pROC: an open-source package for R and S+ to analyze and compare ROC curves. *BMC Bioinformatics* 2011;**12**:77. https://doi.org/10.1186/1471-2105-12-77
22. Machado D, Andrejev S, Tramontano M. *et al.* Fast automated reconstruction of genome-scale metabolic models for microbial species and communities. *Nucleic Acids Res* 2018;**46**:7542–53. https://doi.org/10.1093/nar/gky537
23. Noronha A, Modamio J, Jarosz Y. *et al.* The virtual metabolic human database: integrating human and gut microbiome metabolism with nutrition and disease. *Nucleic Acids Res* 2019;**47**:D614–24. https://doi.org/10.1093/nar/gky992
24. Eddy SR. Accelerated profile HMM searches. *PLoS Comput Biol* 2011;**7**:e1002195. https://doi.org/10.1371/journal.pcbi.1002195
25. Horan K, Shelton CR, Girke T. Predicting conserved protein motifs with sub-HMMs. *BMC Bioinformatics* 2010;**11**:205. https://doi.org/10.1186/1471-2105-11-205
26. Liu Y, Jarman JB, Low YS. *et al.* A widely distributed gene cluster compensates for uricase loss in hominids. *Cell* 2023;**186**:3400–3413.e20. https://doi.org/10.1016/j.cell.2023.06.010
27. Liu C, Cui Y, Li X. *et al.* Microeco: an R package for data mining in microbial community ecology. *FEMS Microbiol Ecol* 2021;**97**:fiaa255. https://doi.org/10.1093/femsec/fiaa255
28. Oksanen J, Simpson GL, Blanchet FG. *et al. Vegan: Community Ecology Package*. 2024. Available at: https://github.com/vegandevs/vegan (3 May 2024, date last accessed).
29. MicrobiotaProcess: a comprehensive R package for deep mining microbiome—ScienceDirect.
30. Breiman L. Random forests. *Mach Learn* 2001;**45**:5–32. https://doi.org/10.1023/A:1010933404324
31. Lu Y, Zhou G, Ewald J. *et al.* Microbiome Analyst 2.0: comprehensive statistical, functional and integrative analysis of microbiome data. *Nucleic Acids Res* 2023;**51**:W310–8. https://doi.org/10.1093/nar/gkad407
32. Manor O, Dai CL, Kornilov SA. *et al.* Health and disease markers correlate with gut microbiome composition across thousands of people. *Nat Commun* 2020;**11**:5206. https://doi.org/10.1038/s41467-020-18871-1
33. Abosamak NR, Gupta V. *Vitamin B6 (Pyridoxine)*. Stat Pearls, 2024. Available at: https://www.ncbi.nlm.nih.gov/books/NBK557436/ (3 April 2024, date last accessed).
34. Lopez MJ, Mohiuddin SS. *Biochemistry, Essential Amino Acids*. Stat Pearls, 2024. Available at: https://www.ncbi.nlm.nih.gov/books/NBK557845/ (3 April 2024, date last accessed).
35. Hinzpeter F, Tostevin F, Gerland U. Regulation of reaction fluxes via enzyme sequestration and co-clustering. *J R Soc Interface* 2019;**16**:20190444. https://doi.org/10.1098/rsif.2019.0444
36. Sun Y, Ma Y, Lin P. *et al.* Fecal bacterial microbiome diversity in chronic HIV-infected patients in China. *Emerg Microbes Infect* 2016;**5**:1–7. https://doi.org/10.1038/emi.2016.25
37. Moon J-Y, Zolnik CP, Wang Z. *et al.* Gut microbiota and plasma metabolites associated with diabetes in women with, or at high risk for, HIV infection. *EBioMedicine* 2018;**37**:392–400. https://doi.org/10.1016/j.ebiom.2018.10.037
38. Rocafort M, Noguera-Julian M, Rivera J. *et al.* Evolution of the gut microbiome following acute HIV-1 infection. *Microbiome* 2019;**7**:73. https://doi.org/10.1186/s40168-019-0687-5
39. Ling Z, Jin C, Xie T. *et al.* Alterations in the fecal microbiota of patients with HIV-1 infection: an observational study in a Chinese population. *Sci Rep* 2016;**6**:30673. https://doi.org/10.1038/srep30673
40. Canfield C-A, Bradshaw PC. Amino acids in the regulation of aging and aging-related diseases. *Transl Med Aging* 2019;**3**:70–89. https://doi.org/10.1016/j.tma.2019.09.001
41. Czibik G, Mezdari Z, Murat Altintas D. *et al.* Dysregulated phenylalanine catabolism plays a key role in the trajectory of cardiac aging. *Circulation* 2021;**144**:559–74. https://doi.org/10.1161/CIRCULATIONAHA.121.054204
42. Gao J, Xu K, Liu H. *et al.* Impact of the gut microbiota on intestinal immunity mediated by tryptophan metabolism. *Front Cell Infect Microbiol* 2018;**8**:13. https://doi.org/10.3389/fcimb.2018.00013
43. Gostner JM, Becker K, Kurz K. *et al.* Disturbed amino acid metabolism in HIV: association with neuropsychiatric symptoms. *Front Psych* 2015;**6**:97.
44. Jiang X, Gao Z, Sharma PP. *et al.* Discovery of low-molecular-weight phenylalanine derivatives as novel HIV capsid modulators with improved antiretroviral activity and metabolic stability. *J Med Virol* 2024;**96**:e29594. https://doi.org/10.1002/jmv.29594
45. Fernstrom JD, Fernstrom MH. Tyrosine, phenylalanine, and catecholamine synthesis and function in the brain. *J Nutr* 2007;**137**:1539S–47 discussion 1548S. https://doi.org/10.1093/jn/137.6.1539S
46. Nolan R, Gaskill PJ. The role of catecholamines in HIV neuropathogenesis. *Brain Res* 2019;**1702**:54–73. https://doi.org/10.1016/j.brainres.2018.04.030
47. Mason S, van Reenen M, Rossouw T. *et al.* Phenylalanine metabolism and tetrahydrobiopterin bio-availability in COVID-19 and HIV. *Heliyon* 2023;**9**:e15010. https://doi.org/10.1016/j.heliyon.2023.e15010
48. Xu S, Sun L, Barnett M. *et al.* Discovery, crystallographic studies, and mechanistic investigations of novel phenylalanine derivatives bearing a quinazolin-4-one scaffold as potent HIV capsid modulators. *J Med Chem* 2023;**66**:16303–29. https://doi.org/10.1021/acs.jmedchem.3c01647
49. Nazli A, Chan O, Dobson-Belaire WN. *et al.* Exposure to HIV-1 directly impairs mucosal epithelial barrier integrity allowing microbial translocation. *PLoS Pathog* 2010;**6**:e1000852. https://doi.org/10.1371/journal.ppat.1000852
50. Hirao LA, Grishina I, Bourry O. *et al.* Early mucosal sensing of SIV infection by Paneth cells induces IL-1β production and initiates gut epithelial disruption. *PLoS Pathog* 2014;**10**:e1004311. https://doi.org/10.1371/journal.ppat.1004311
51. Hunt PW, Sinclair E, Rodriguez B. *et al.* Gut epithelial barrier dysfunction and innate immune activation predict mortality in treated HIV infection. *J Infect Dis* 2014;**210**:1228–38. https://doi.org/10.1093/infdis/jiu238
52. Gootenberg DB, Paer JM, Luevano J-M. *et al.* HIV-associated changes in the enteric microbial community: potential role in loss of homeostasis and development of systemic inflammation. *Curr Opin Infect Dis* 2017;**30**:31–43. https://doi.org/10.1097/QCO.0000000000000341
53. Kaur US, Shet A, Rajnala N. *et al.* High abundance of genus Prevotella in the gut of perinatally HIV-infected children is associated with IP-10 levels despite therapy. *Sci Rep* 2018;**8**:17679. https://doi.org/10.1038/s41598-018-35877-4
54. Zhou J, Zhang Y, Cui P. *et al.* Gut microbiome changes associated with HIV infection and sexual orientation. *Front Cell Infect Microbiol* 2020;**10**:434. https://doi.org/10.3389/fcimb.2020.00434
55. Sperk M, Ambikan AT, Ray S. *et al.* Fecal metabolome signature in the HIV-1 elite control phenotype: enrichment of dipeptides acts as an HIV-1 antagonist but a Prevotella agonist. *J Virol* 2021;**95**:e0047921. https://doi.org/10.1128/JVI.00479-21
56. Innocenti GP, Santinelli L, Laghi L. *et al.* Modulation of phenylalanine and tyrosine metabolism in HIV-1 infected patients with neurocognitive impairment: results from a clinical trial. *Metabolites* 2020;**10**:274. https://doi.org/10.3390/metabo10070274

57. Villanueva-Millán MJ, Pérez-Matute P, Recio-Fernández E. *et al.* Differential effects of antiretrovirals on microbial translocation and gut microbiota composition of HIV-infected patients. *J Int AIDS Soc* 2017;**20**:21526. https://doi.org/10.7448/IAS.20.1.21526
58. Roiser JP, McLean A, Ogilvie AD. *et al.* The subjective and cognitive effects of acute phenylalanine and tyrosine depletion in patients recovered from depression. *Neuropsychopharmacol Off Publ Am Coll Neuropsychopharmacol* 2005;**30**:775–85. https://doi.org/10.1038/sj.npp.1300659
59. Taylor BC, Weldon KC, Ellis RJ. *et al.* Reduced independence in daily living is associated with the gut microbiome in people with HIV and HCV. *mSystems* 2020;**5**:e00528–0. https://doi.org/10.1128/mSystems.00528-20
60. Saji N, Niida S, Murotani K. *et al.* Analysis of the relationship between the gut microbiome and dementia: a cross-sectional study conducted in Japan. *Sci Rep* 2019;**9**:1008. https://doi.org/10.1038/s41598-018-38218-7
61. Wang R, Zheng X, Song F. *et al.* Deciphering associations between gut microbiota and clinical factors using microbial modules. *Bioinformatics* 2023;**39**:btad213. https://doi.org/10.1093/bioinformatics/btad213
62. Wang B, Sun F, Luan Y. Comparison of the effectiveness of different normalization methods for metagenomic cross-study phenotype prediction under heterogeneity. *Sci Rep* 2024;**14**:7024. https://doi.org/10.1038/s41598-024-57670-2

Briefings in Bioinformatics, 2025, **26(2)**, bbaf111
https://doi.org/10.1093/bib/bbaf111
Case Study